Int. J. Heat Mass Transfer. Vol. 27, No. 3, pp. 409–417, 1984
Printed in Great Britain

0017-9310/84 $3.00 + 0.00

TEMPERATURE DISTRIBUTIONS AROUND BURIED PIPE NETWORKS IN SOIL WITH A TEMPERATURE DEPENDENT THERMAL CONDUCTIVITY

ABRAHAM DAYAN and ALAN H. MERBAUM†
Department of Fluid Mechanics and Heat Transfer, Tel Aviv University, School of Engineering, Ramat Aviv 69978, Israel

and

ISHAIAHU SEGAL
Agricultural Research Organization/Institute of Agricultural Engineering, P.O.B. 6, Bet Dagan 50200, Israel

(*Received* 12 *July* 1982 *and in revised form* 27 *June* 1983)

Abstract—The temperature distribution in soil around a network of subsurface horizontal warm water pipes was investigated. Computations of soil thermal conductivity revealed a linear dependence on temperature due to the presence of moisture and induced vapour diffusion within the pore space. Solutions of the temperature distributions around various buried pipe networks were obtained in closed forms and numerically. Experiments were conducted with a single buried pipe. The data showed that the present model yields better predictions than previous constant property models. Analyses were extended to account for effects of desiccation around the heated pipes. The results are applicable in horticulture for improved designs of soil warming networks.

NOMENCLATURE

a, b	coefficients of the thermal conductivity function
$\bar{a}, \bar{b}$	dimensionless parameters defined after equation (15)
c_p	specific heat
d	depth of buried pipes
D	mass diffusivity
f	dimensionless layout function
F_j, G_j	dimensionless functions, defined by equations (30) and (31)
g	depolarization factor of an ellipsoid
h_{fg}	specific latent heat
j	mass flux
J	constituent parameter, defined by equation (39)
k	thermal conductivity
L	pipe length
$\dot{m}$	mass flow rate
M	total number of soil constituents
$\bar{M}$	molecular weight
n	index for counting pipes
N	number of influencing pipes in each direction
p	pressure
P	dimensionless function, defined after equation (13)
$\dot{q}$	heat flux leaving a unit length of pipe
$\ddot{q}$	heat flux per unit area
Q	dimensionless heat flux, defined after equation (13)
r	radial coordinate
R	pipe radius
$\bar{R}$	universal gas constant
s	distance between pipes
T	temperature
x, y, z	Cartesian coordinates.

Greek symbols (all dimensionless)

α	angle
β	design parameter
γ	parameter, defined after equation (32)
η_1, η_2	functions, defined after equation (32)
θ	transformed temperature, defined by equation (8)
λ	parameter, defined after equation (32)
μ	parameter, defined after equation (18)
ν	parameter, $\bar{a}/2\bar{b}$
ϕ	relative humidity
ψ	parameter, defined after equation (19)
ω	volume fraction of a soil constituent.

Subscripts

a	air
abs	absolute
app	apparent
cr	critical
d	dry
f	field capacity
i	interface
i	constituent
in	inlet
j	index of functions
l, m, n	axes of ellipsoid
p	probe
s	surface
v	vapour

† Present address: Syska and Hennessy Engineers, Inc., 575 Mission Street, San Francisco, CA 94105, U.S.A.

w wall
w water
0 parallel flow system
1, 2 counterdirectional flow system.

Superscripts
s saturated
~ dimensionless
' dummy variable
* transformed temperature, defined by equation (7).

1. INTRODUCTION

SOIL warming in horticulture is a method for increasing crop yield and growth rates [1–4]. It is an attractive alternative to conventional heating techniques because it relies on low temperature energy sources, such as industrial waste heat, geothermal and solar energy [4–6]. More efficient agricultural management and utilization of low temperature waste heat are also important contributions to environmental protection.

Energy transport in soil is generally coupled with mass transfer [7, 8]. The moisture distribution in a soil is affected by irrigation conditions, the soil's physical properties, presence of solutions in the soil water, crop induced effects, gravity, hysteresis effects, and temperature gradients [8–12]. It is complex to incorporate all these variables in system design studies. Furthermore, the lack of data on material properties is a major obstacle in implementation of elaborate models. Consequently, models have been developed for idealized or limiting conditions. Among the simplifications often used is the assumption of constant thermal properties [13–16].

The present work was undertaken with the purpose of developing a useful model which would account for vapour transport effects. Vapour diffusion within the pore space is a powerful mechanism of latent heat energy transport. In general, the process is driven by temperature and moisture gradients [10, 17, 18]. However, inspection of studies on energy transport in soil around buried cables and heated pipes reveals the dominant role of temperature gradients [4, 19–21]. Under steady-state conditions, moisture gradients are mainly important in areas where the fluxes of vapour and moisture are comparable in magnitude and in opposite directions [8, 18, 22]. Such conditions could form in the immediate vicinity of heated pipes and cables at temperatures well above 40°C. They are associated with desiccation of the soil near the heat source, a phenomenon which can be expected only if heat fluxes are excessive [8, 19, 22]. Owing to the limitation it presents for soil warming, the influence of soil desiccation is analysed in Appendix I.

The proposed model is concerned with the energy transport from a network of buried parallel pipes. Energy transfer is assumed to be mainly driven by temperature gradients at rates which depend on an average moisture content. This condition applies to both moist soils (with relative humidity close to unity) and soils of low moisture content [12]. In both, moisture distributions and gradients are of little effect. Soils with desiccated zones around the pipes are modelled in Appendix I as two zone regions with respect to the local average moisture content. All of the above conditions are of particular importance to designers since they reveal limits of root zone temperatures and heating system capacities. Moreover, the model can be used to study soils with intermediate moisture contents when the soil properties and conditions are such that moisture distributions are likely to be nearly uniform [4, 21, 22].

Analytical and numerical solutions describing the temperature field around a single pipe or network of parallel pipes are presented. Experiments were conducted to test the model. Results are applicable to other engineering and bioengineering [23] problems involving surface cooling or heating by a system of substrate parallel pipes.

2. PHYSICAL MODEL

Consider a soil heated by a system of warm parallel pipes buried at a depth d beneath the soil surface a distance s apart, as shown in Fig. 1. The flow of water in adjacent pipes may be either cocurrent or countercurrent. The temperature at the soil surface and deep in the soil is assumed to be constant and equal to the average diurnal temperature. The diurnal cycle influences the temperature of a shallow layer of soil and is of little effect at deeper depths [24]. Therefore, calculated temperature distributions are in effect time averaged distributions.

Conservation of energy in a soil under steady-state conditions with negligible gravitational effects is described by

$$\nabla(k_d \nabla T) + h_{fg} \nabla j_v = 0, \tag{1}$$

where the vector of the vapour mass flow rate is given by

$$j_v = -D[p/(p-p_v)]\,[\bar{M}/(\bar{R}T_{abs})]\,\nabla(\phi p_v^s), \tag{2}$$

and D is the vapour diffusivity in the pore system which is dependent on tortuosity, porosity, moisture content and temperature [10]. The relative humidity, ϕ, is

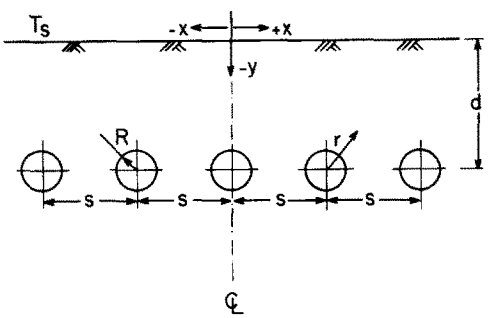

FIG. 1. Cross-sectional view of underground soil warming network.

primarily affected by moisture content, whereas saturation pressure is affected by temperature. Therefore, expansion of the last term of equation (2) gives

$$\nabla(\phi p_v^s) = \phi \frac{dp_v^s}{dT} \frac{(\nabla T)_a}{\nabla T} \nabla T + p_v^s \frac{d\phi}{d\omega_v} \nabla \omega_v, \quad (3)$$

where $(\nabla T)_a$ denotes temperature gradients in the air filled pores. In both moist and relatively dry soils the temperature gradient term is dominant [8, 12, 18]. Therefore, analyses are often based on the simplified form of equation (1) assuming that moisture effects can be adequately represented by incorporating an average value of moisture content [4, 17, 20]

$$\nabla(k_d \nabla T) + \nabla\left[h_{fg} \phi k_v^s \frac{(\nabla T)_a}{\nabla T} \nabla T\right] = \nabla(k \nabla T). \quad (4)$$

The resultant apparent thermal conductivity is dependent on temperature and moisture content. The temperature sensitivity is primarily a consequence of latent heat transport by vapour diffusion within the pore space (evaporation and diffusion towards recondensation in colder regions). This intense mechanism of energy transfer is more progressive at higher temperatures [9]. Consequently, the overall thermal conductivity for the combined effects of sensible and latent heat transfer is an increasing function of temperature.

A method for calculating the apparent thermal conductivity as a function of temperature and moisture content is described in Appendix II. The results show that the thermal conductivity can be approximated by a linear function

$$k = aT + b, \quad (5)$$

with coefficients dependent on soil properties and averaged moisture content.

The temperature field in a field heated by a system of parallel pipes is three dimensional. Nevertheless, only two derivative terms of equation (4) must be retained. For effectively heating the soil, the heating fluid temperature throughout the field length should remain above ambient temperatures. Therefore, an order of magnitude comparison between the various terms of equation (4) reveal

$$O\left\{\frac{\partial^2 T}{\partial z^2} \Big/ \frac{\partial^2 T}{\partial y^2}\right\} = d^2/L^2 \ll 1,$$

which indicates that conduction in the z-direction can be neglected. The nonuniformity of the soil axial temperature distribution results from the longitudinal temperature drop of the heating fluid. The equation to be solved is therefore

$$\frac{\partial}{\partial x}\left(k \frac{\partial T}{\partial x}\right) + \frac{\partial}{\partial y}\left(k \frac{\partial T}{\partial y}\right) = 0. \quad (6)$$

This equation is nonlinear since it contains a temperature-dependent thermal conductivity. A linear equation can be derived following the definition of a new variable, which is

$$T^* = \int_{T'=0}^{T} k(T')\, dT'. \quad (7)$$

It is advantageous to nondimensionalize the equations by introducing the following dimensionless quantities

$$\begin{aligned} \theta(\bar{x}, \bar{y}, \bar{z}) &= (T^* - T_s^*)/(T_{in}^* - T_s^*), \\ \bar{x} &= x/d, \\ \bar{y} &= y/d, \\ \bar{z} &= z/L. \end{aligned} \quad (8)$$

The resultant linear equation in terms of θ is

$$\frac{\partial^2 \theta}{\partial \bar{x}^2} + \frac{\partial^2 \theta}{\partial \bar{y}^2} = 0, \quad (9)$$

with boundary conditions:

$$\begin{aligned} \theta(\bar{x}, 0, \bar{z}) &= 0, \\ \theta(\pm\infty, \bar{y}, \bar{z}) &= 0, \\ \theta(\bar{x}, -\infty, \bar{z}) &= 0, \\ \theta &= \theta_w(\bar{z}) \quad \text{(on the pipe wall)}. \end{aligned} \quad (10)$$

The last boundary condition couples the energy transport in the soil to the energy convected through the pipes.

Thermal conductivity of pipe material and water are much greater than that of a soil. Therefore, negligible temperature gradients are expected within any cross section of the pipe. The pipe wall axial temperature distribution is obtained from an energy balance, i.e.

$$\dot{m} c_p \frac{dT_w}{d\bar{z}} + \dot{q} = 0, \quad (11)$$

and

$$\dot{q} = -R \int_0^{2\pi} \left[k \frac{\partial T}{\partial r}\right]_{r=R} d\alpha. \quad (12)$$

Equation (12) designates the rate of energy loss per unit length of pipe. In a dimensionless form, equation (11) appears as

$$\frac{d\theta_w}{d\bar{z}} + QP = 0, \quad (13)$$

where

$$\begin{aligned} Q &= Q(\theta_w) = \dot{q}/(T_{in}^* - T_s^*), \\ P &= P(\theta_w) = Lk/\dot{m} c_p. \end{aligned}$$

The pipe wall temperature is subject to the boundary condition

$$\theta_w(0) = 1. \quad (14)$$

The dimensionless dependence of k on θ is obtained by combining equations (5), (7) and (8) which yields

$$\bar{k} = (\bar{a}\theta + \bar{b})^{1/2}, \quad (15)$$

with

$$\bar{k} = k/b,$$

$$\bar{a} = (2a/b^2)(T^*_{in} - T^*_s),$$

$$\bar{b} = 1 + (2a/b^2)T^*_s.$$

3. TEMPERATURE AROUND A SINGLE BURIED PIPE

The solution of equation (9) is based on the image technique. Solutions of a line source and a line sink are superimposed. The source and sink are placed at equal distances above and below the soil surface [24]. This yields the dimensionless transformed temperature field around a single buried pipe subject to the boundary conditions, equation (10)

$$\theta = \frac{Q}{4\pi} \ln\left[\frac{\bar{x}^2 + (1-\bar{y})^2}{\bar{x}^2 + (1+\bar{y})^2}\right]. \tag{16}$$

The lines of constant θ are circular. The contour defined by one of these lines can be identified as the pipe wall, as seen in Fig. 2. For simplicity, it is assumed that the pipe wall temperature coincides with the temperature at $x = 0$ and $y = R - d$. Thus

$$\theta_w = \theta(0, \bar{R} - 1, \bar{z}) = \frac{Q}{2\pi} \ln[(2/\bar{R}) - 1]. \tag{17}$$

Combining equations (13), (15) and (17) gives the equation that describes $\theta_w(\bar{z})$

$$\left(\frac{\bar{a}}{\bar{b}}\theta_w + 1\right)^{-1/2} \frac{d\theta_w}{d\bar{z}} + 2\beta\theta_w = 0, \tag{18}$$

where

$$\mu = \frac{\pi b L}{\dot{m} c_p}\left[1 + \left(\frac{2a}{b^2}\right)T^*_s\right]^{1/2},$$

$$\beta = \mu/\ln[(2/\bar{R}) - 1].$$

The solution of this equation with the boundary condition at $\bar{z} = 0$ is

$$\theta_w = (\bar{b}/\bar{a})[\coth^2(\coth^{-1}\psi + \beta\bar{z}) - 1], \tag{19}$$

with

$$\psi = [1 + (\bar{a}/\bar{b})]^{1/2}.$$

Equations (16), (17) and (19) constitute the solution of the single pipe problem. The dimensional temperatures can be retrieved by using equation (8) to obtain T^*, and the integrated form of equation (7) to obtain T.

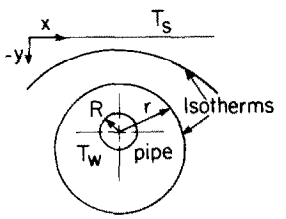

FIG. 2. Lines of constant temperature around a single buried pipe.

4. UNIDIRECTIONAL FLOW SYSTEM

Consideration is first directed to a system of buried pipes in which water is flowing cocurrently. The transformed dimensionless temperature field for this system can be constructed from the solution of the single buried pipe. Neglecting end field effects, the temperature distribution around a pipe would be affected only by a finite number of pipes (N) on each side. Superposition of solutions for the pipe at $x = 0$ gives

$$\theta = \frac{Q}{4\pi}\left\{\sum_{n=0}^{N} \ln\left[\frac{(n\bar{s} + \bar{x})^2 + (1-\bar{y})^2}{(n\bar{s} + \bar{x})^2 + (1+\bar{y})^2}\right] + \sum_{n=1}^{N} \ln\left[\frac{(n\bar{s} - \bar{x})^2 + (1-\bar{y})^2}{(n\bar{s} - \bar{x})^2 + (1+\bar{y})^2}\right]\right\}, \tag{20}$$

where $\bar{s}$ is the dimensionless distance between adjacent pipes ($\bar{s} = s/d$). Furthermore, by identifying the pipe wall with the nearly circular isotherm that runs through $\bar{y} = \bar{R} - 1$, one gets

$$\theta_w = \frac{Q}{2\pi} f, \tag{21}$$

where

$$f = \ln\left(\frac{2}{\bar{R}} - 1\right) + \sum_{n=1}^{N} \ln\left[\frac{(n\bar{s})^2 + (2-\bar{R})^2}{(n\bar{s})^2 + \bar{R}^2}\right].$$

Substituting $Q(\theta_w)$ from equation (21) into equation (13) and solving for θ_w, subject to the boundary condition at $\bar{z} = 0$, yields

$$\theta_w = (\bar{b}/\bar{a})[\coth^2(\coth^{-1}\psi + \beta_0\bar{z}) - 1], \tag{22}$$

where

$$\beta_0 = \mu/f.$$

Equations (22) and (19) would have been identical if not for the definition of β. Since β_0 is smaller than β, the pipe wall temperature of the unidirectional flow system is larger than that of a single buried pipe, as expected.

5. COUNTERDIRECTIONAL FLOW SYSTEM

In the counterdirectional flow system, water is flowing countercurrently in neighbouring pipes. At any $\bar{z}$ location, the temperature of pipes containing a flow in one direction (group 1) would be different from the temperature of pipes with an opposite flow direction (group 2). Likewise, the local heat fluxes leaving the two groups of pipes would be different. Thus, the solution of the θ field

$$\theta = \frac{Q_1}{4\pi}\left\{\sum_{n=0}^{N/2} \ln\left[\frac{(2n\bar{s} + \bar{x})^2 + (1-\bar{y})^2}{(2n\bar{s} + \bar{x})^2 + (1+\bar{y})^2}\right] + \sum_{n=1}^{N/2} \ln\left[\frac{(2n\bar{s} - \bar{x})^2 + (1-\bar{y})^2}{(2n\bar{s} - \bar{x})^2 + (1+\bar{y})^2}\right]\right\} + \frac{Q_2}{4\pi}\left\{\sum_{n=1}^{N/2} \ln\left[\frac{[(2n-1)\bar{s} + \bar{x}]^2 + (1-\bar{y})^2}{[(2n-1)\bar{s} + \bar{x}]^2 + (1+\bar{y})^2}\right] + \sum_{n=1}^{N/2} \ln\left[\frac{[(2n-1)\bar{s} - \bar{x}]^2 + (1-\bar{y})^2}{[(2n-1)\bar{s} - \bar{x}]^2 + (1+\bar{y})^2}\right]\right\}, \tag{23}$$

contains two dimensionless heat fluxes, Q_1 and Q_2, which are yet to be determined. Identifying the pipes' walls with the isotherms that run at $\bar{y} = \bar{R} - 1$ and right above each pipe centreline gives

$$\theta_{w1} = \frac{Q_1}{2\pi} f_1 + \frac{Q_2}{2\pi} f_2, \tag{24}$$

$$\theta_{w2} = \frac{Q_1}{2\pi} f_2 + \frac{Q_2}{2\pi} f_1, \tag{25}$$

where

$$f_1 = \ln\left(\frac{2}{\bar{R}} - 1\right) + \sum_{n=1}^{N/2} \ln\left[\frac{(2n\bar{s})^2 + (2-\bar{R})^2}{(2n\bar{s})^2 + \bar{R}^2}\right],$$

$$f_2 = \sum_{n=1}^{N/2} \ln\left[\frac{[(2n-1)\bar{s}]^2 + (2-\bar{R})^2}{[(2n-1)\bar{s}]^2 + \bar{R}^2}\right].$$

Solving the equation for θ_{w1} and θ_{w2} and substituting the results in equation (13) yields a pair of coupled energy equations

$$\left(\frac{\bar{a}}{\bar{b}}\theta_{w1} + 1\right)^{-1/2} \frac{d\theta_{w1}}{d\bar{z}} + 2(\beta_1\theta_{w1} - \beta_2\theta_{w2}) = 0, \tag{26}$$

$$\left(\frac{\bar{a}}{\bar{b}}\theta_{w2} + 1\right)^{-1/2} \frac{d\theta_{w2}}{d\bar{z}} - 2(\beta_1\theta_{w2} - \beta_2\theta_{w1}) = 0, \tag{27}$$

with

$$\beta_1 = \frac{\mu f_1}{f_1^2 - f_2^2},$$

$$\beta_2 = \frac{\mu f_2}{f_1^2 - f_2^2}.$$

The boundary conditions are:

$$\theta_{w1}(0) = 1, \tag{28}$$

$$\theta_{w2}(1) = 1. \tag{29}$$

Equations (26) and (27) were integrated numerically. The numerical procedure was based on searching the value of θ_{w2} that would yield after integration the symmetry condition $\theta_{w1} = \theta_{w2}$. Notice that the equations explicitly provide the values of θ_{w1} and θ_{w2} at $z + \Delta z$ once they are known at z.

Expanding the term $(\bar{a}\theta_w/\bar{b} + 1)^{-1/2}$ in a Taylor series enabled the development of an asymptotic solution. When the parameter $v (= \bar{a}/2\bar{b})$ is small, the solution has the form of

$$\theta_{w1}(\bar{z}) = F_0 + vF_1 + v^2F_2 + \ldots, \tag{30}$$

$$\theta_{w2}(\bar{z}) = G_0 + vG_1 + v^2G_2 + \ldots. \tag{31}$$

The individual functions, F_i and G_i, are obtained from the solution of a sequence of coupled pairs of differential equations. This follows the substitution of equations (30) and (31) into equations (26) and (27) subject to the boundary conditions (28) and (29). The results for the first two terms are

$$\theta_{w1}(\bar{z}) = \{1 - v[\eta_1 + \eta_2 \exp(2\lambda)]\} \times \left\{\frac{\exp(\lambda\bar{z}) + \gamma \exp[\lambda(1-\bar{z})]}{1 + \gamma \exp(\lambda)}\right\} + v\{\eta_1 \exp(2\lambda\bar{z}) + \eta_2 \exp[2\lambda(1-\bar{z})]\}, \tag{32}$$

$$\theta_{w2}(\bar{z}) = \theta_{w1}(1-\bar{z}), \tag{33}$$

where

$$\gamma = [\beta_1 + (\beta_1^2 + \beta_2^2)^{1/2}]/\beta_2,$$

$$\lambda = 2(\beta_1^2 - \beta_2^2)^{1/2},$$

$$\eta_1 = (2\gamma^2 + 3\gamma + 3)/\{3(1+\gamma)[1 + \gamma \exp(\lambda)]^2\},$$

$$\eta_2 = (3\gamma^2 + 3\gamma + 2)\gamma/\{3(1+\gamma)[1 + \gamma \exp(\lambda)]^2\}.$$

The numerical solution or the asymptotic solution can be utilized to calculate the dimensionless heat fluxes of equation (23) via equations (24) and (25).

The boundary conditions set by equations (28) and (29) suit a heating system with four manifolds, two on each side of the field. It is possible to reduce the system to two manifolds with a loop type flow. This would require connecting the pipes in pairs at the end of the field. The pertinent boundary condition for this configuration is $\theta_{w1} = \theta_{w2}$. Owing to symmetry, the solution for a field of length L with the boundary conditions of equations (28) and (29) would apply to a loop type field of length $L/2$.

6. RESULTS AND DISCUSSION

Dimensionless pipe wall temperature distributions for the three heating configurations are plotted in Fig. 3. The results are for a heating system 1.6 cm in diameter, 100 m long, 40 cm apart and at a depth of 40 cm. The inlet temperature of the heating fluid is 55°C and the flow rate is 0.02 kg s^{-1}. The field surface temperature is 15°C and the thermal conductivity, in W m^{-1} °C^{-1}

$$k(T) = 0.0277T + 0.323. \tag{34}$$

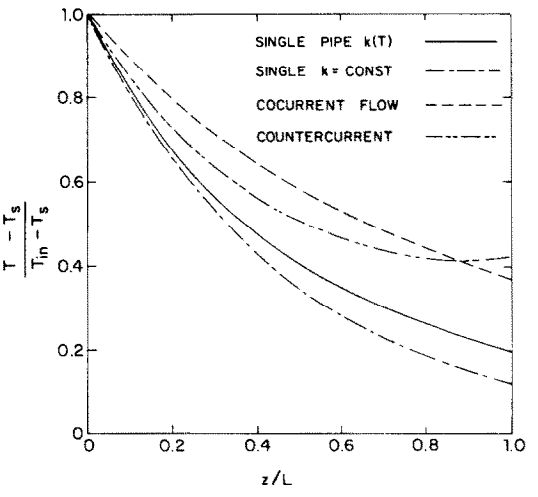

FIG. 3. Dimensionless pipe wall temperature distributions.

The counterdirectional flow system induces a fairly uniform temperature distribution over a large portion of the field, especially when considering average conditions between two adjacent pipes. Therefore, this is the agriculturally most attractive system. The rise of the temperature towards $\bar{z} = 1$ indicates that near the outlet the fluid gains heat from the two neighbouring pipes. For comparison, the results for a single heating pipe assuming a constant average thermal conductivity, evaluated at $(T_{in} + T_s)/2$, were added to the figure. It is seen that heating requirements as predicted by the constant property model, for the given conditions, are overpredicted by about 10%. This results from excessive heat dissipation around the colder section of the pipe, a region where the real thermal conductivity is lower than the average conductivity.

Soil temperature distributions in planes of constant z are similar in shape to those of constant property fields [13]. For a single heating pipe this can be observed in Fig. 4. Figure 4 also contains experimental data obtained from an experiment which was conducted in a 1/4 acre greenhouse located south of Rehovot, Israel.

In the experiment [24], a 10 m, $\frac{1}{2}$ in. (12.7 mm) galvanized steel pipe was buried 26 cm beneath the soil surface. The soil consisted of 95% sand and 5% organic matter. A thermocouple array was assembled 8 m from the water inlet. Data was recorded hourly by a 20 point Doric automatic recorder for 92 h, beginning at 10.00 a.m. on 14 April 1980. For the soil medium considered, a field capacity of 0.08, moisture content of 0.035 and porosity of 0.45 were assumed. The thermal conductivity of the sand was evaluated by the method described in Appendix II. Calculated values of conductivity and their linear representation are shown in Fig. 5.

Comparison between measured and predicted temperatures favours the temperature dependent thermal conductivity model. In the vicinity of the heating pipe, isotherms of the constant conductivity model indicate steeper than measured temperature gradients. Insensitivity of the model to the local higher thermal conductivity is the source of the discrepancy.

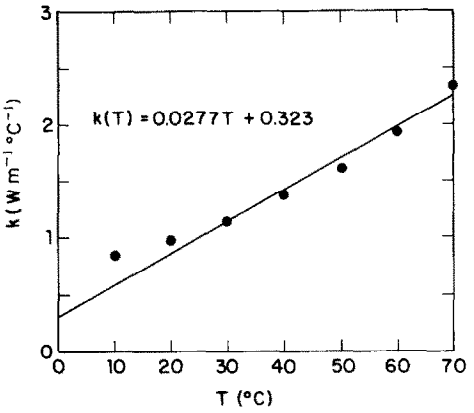

FIG. 5. Thermal conductivity expressed as a function of temperature for Ramot Meir sand.

In the limit, results of the variable conductivity model reduce to those of the constant conductivity model [24]. A graphical design procedure to satisfy soil warming demands has been presented in refs. [24, 25]. It provides a simple way to select the appropriate design parameters, β_i's, for given layout parameters, f_i's. Notice that the β parameters designate the ability of a system to give up heat relative to its capacity.

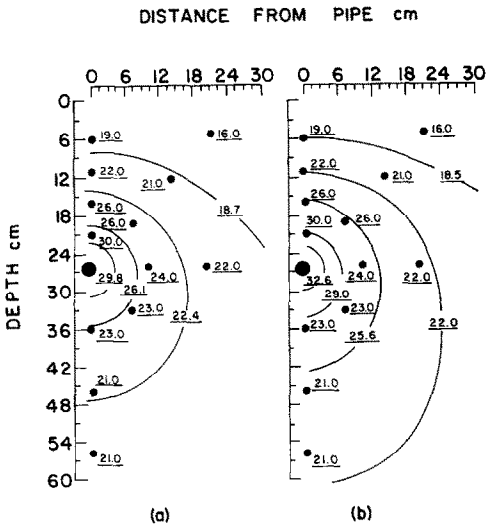

FIG. 4. Comparison of (a) constant property and (b) variable property models with measured data at 8 m from pipe inlet.

7. CONCLUDING REMARKS

Considering the nonlinearity of the problem, the model presented offers a simple tool for calculating a three dimensional temperature distribution of a heated soil. By accounting for vapour transport effects, improved predictions of experimental data were obtained as compared to predictions of a widely used model [13].

The soil thermal conductivity in the low moisture range exhibits a strong dependence on temperature. This yields the greatest shift of local temperature distributions from conditions of constant properties under the same boundary conditions and moisture content. The present model can be used to calculate such extreme root zone temperatures. This also applies to conditions of high moisture content, where the soil is highly conductive and the energy fluxes are greatest. Calculations of a heating system capacity should be performed for such conditions. From theoretical considerations the required dependence of thermal conductivities on temperature can be obtained with an accuracy of 10%. When based on minimal experimental data, the accuracy is doubled.

REFERENCES

1. W. W. Brown and D. P. Ormrod, Response of the chrysanthemum to soil heating, *Scienta Horticulturae* **13**, 67–75 (1980).
2. W. W. Brown and D. P. Ormrod, Soil temperature effects

on greenhouse roses in relation to air temperature and nutrition, *J. Am. Soc. Hort. Sci.* **105,** 57–59 (1980).
3. A. J. Cooper, Root temperature and plant growth, Commonwealth Bureau of Horticulture and Plantation Crops, Commonwealth Agriculture Bureau, Farnham Royal, Slough S12 3BN, U.K. (1973).
4. W. L. Roller and D. L. Elwell, Greenhouse soil heating for improved production and energy conservation, Electric Power Research Institute, EPRI-EA-2022, Project 1110-1, Final Report (1981).
5. J. E. Alpert, S. C. VanDemark, D. D. Fritton and D. R. DeWalle, Soil temperature and heat loss for a hot water pipe network buried in irrigated soil, *J. Environ. Qual.* **5,** 400–405 (1976).
6. L. Boersma and K. A. Rykbost, Integrated systems for utilizing waste heat from steam generating plants, *J. Environ. Qual.* **2,** 179–188 (1973).
7. J. R. Phillip and D. A. DeVries, Moisture movements in porous materials under temperature gradients, *Trans. Am. Geophys. Un.* **38**(2), 222–232 (1957).
8. J. G. Hartley and W. Z. Black, Transient simultaneous heat and mass transfer in moist unsaturated soils, *J. Heat Transfer* **103,** 378–382 (1981).
9. D. A. DeVries, Thermal properties of soils, *Physics of Plant Environment* (edited by W. R. Van Wijk), p. 210. North Holland, Amsterdam (1963).
10. D. A. DeVries, Heat transfer in soils, *Heat and Mass Transfer in the Biosphere—Part 1. Transfer Processes in Plant Environment* (edited by D. A. DeVries and N. H. Afghan). Scripta, Washington, DC (1975).
11. A. Hadas, Evaluation of theoretically predicted thermal conductivities of soils under field and laboratory conditions, *Soil Sci. Soc. Am. J.* **41** (3), 460–466 (1977).
12. A. R. Sepaskhah and L. Boersma, Thermal conductivity of soils as a function of temperature and water content, *Soil Sci. Soc. Am. J.* **45,** 439–444 (1979).
13. J. N. Kendrick and J. A. Havens, Heat transfer models for a subsurface water pipe, soil warming system, *J. Environ. Qual.* **2,** 188–196 (1973).
14. D. L. Slegel and L. R. Davies, Transient heat and mass transfer in soils in the vicinity of heated porous pipes, *J. Heat Transfer* **99,** 541–546 (1977).
15. H. H. Bau and S. S. Sadhal, Heat losses from a fluid flowing in a buried pipe, *Int. J. Heat Mass Transfer* **25,** 1621–1629 (1982).
16. V. M. Puri, Greenhouse floor heating system optimization using long term thermal performance design curves, *Solar Energy* **28**(6), 469–481 (1982).
17. D. W. Westcot and P. J. Wierenga, Transfer of heat by conduction and vapor movement in a closed soil system, *Soil Sci. Soc. Am. Proc.* **38,** 9–14 (1974).
18. D. A. DeVries, Simultaneous transfer of heat and moisture in porous media, *Trans. Am. Geophys. Un.* **39**(5), 909–916 (1958).
19. J. V. Schmill, Discussion on influence of moisture content of soil on buried-cable ratings, *Proc. IEE* **111**(12), 2081–2095 (1964).
20. A. G. Milne and K. Mochlinski, Characteristics of soil affecting cable ratings, *Proc. IEE* **111**(5), 1017–1039 (1964).
21. A. N. Arman, D. M. Cherry, L. Gosland and P. M. Hollingsworth, Influence of soil-moisture migration on power rating of cables in H. V. transmission systems, *Proc. IEE* **111**(5), 1000–1016 (1964).
22. H. S. Radhakrishna, F. Y. Chu and S. A. Boggs, Thermal instability and its prediction on cable backfill soils, *IEEE Trans. Power Apparatus Systems* **PAS-99**(3), 856–863 (1980).
23. J. C. Chato, Heat transfer to blood vessels, *J. Biomech. Engng* **102,** 110–118 (1980).
24. A. H. Merbaum, An analysis of soil warming for agricultural purposes, Masters thesis, Tel Aviv University School of Engineering (1981).
25. A. H. Merbaum, I. Segal and A. Dayan, Design procedures for soil warming systems, *Energy Agriculture* (1984) in press.

APPENDIX I

DESICCATION OF SOIL AROUND THE BURIED HEATED PIPE

Early investigations related the drying of soil around buried cables to a threshold temperature ranging between 30 and 40°C [20, 21]. Recent experimental data, however, showed little or no moisture loss around three types of soils with a pipe temperature of 40°C [4]. Though representing a potential for moisture thermal removal, one must conclude that temperature alone is not the criterion for soil desiccation. Recently published works relate the initiation of desiccation to the critical moisture content [8, 19, 22]. At moisture contents below the critical value, vapour permeability increases to a point such that vapour outflow cannot be compensated by capillary liquid inflow. The same theory suggests that for each initial moisture content and soil properties, there exists a critical heat flow below which desiccation could not commence. Under sustained heating by a constant temperature source the dried region would expand, however, at a continuously decreasing rate owing to both reduced soil conductivity and decreased heat flux around the dry region. The expansion of drying would cease when the heat flow at the periphery of the dry region drops to the critical value. The critical heat flux can be either calculated or measured using the hot probe method [8]. In the latter method the critical heat flux, $\ddot{q}_{cr}$ is related to the probe linear flux $\dot{q}_{cr}$ simply by $\ddot{q}_{cr} = \dot{q}_{cr}/2\pi r_p$.

Experimental investigations showed that desiccated regions around heated cylinders are nearly annular in shape [4, 21]. The boundary between the dry and moist regions could be sharp or gradual, depending on the soil texture [18–20]. In sandy soils the boundary is well defined due to the low capillary tension.

To analyse the influence of drying on the temperature field around a heated pipe it is assumed that the soil can be characterized as a medium having two regions; one dry and the other moist with a suitable uniform moisture content. In addition, the dry region is assumed annular and concentric with the pipe. This is justified in view of the small heat fluxes involved (< 150 W m^{-1}) which cannot thermally expel moisture more than a few centimetres away from the pipe [4].

With the lack of moisture transport effects, the dry-region thermal conductivity can be considered constant. The heat flux leaving the dry region (at the boundary) under steady-state conditions should be equal to the critical heat flux. From the solution of the energy transfer equation for conduction across the dry region

$$r_i \ddot{q}_{cr} \ln\left(\frac{r_i}{R}\right) = k_d(T_w - T_i), \tag{35}$$

where the subscript i denotes interface conditions between the dry and moist zones. From conductivity requirements, the same heat flux must cross the moist region towards dissipation to the atmosphere. Thus

$$r_i q_{cr} \ln[(2d - r_i)/r_i] = \int_{T_s}^{T_i} k(T')\,dT'. \tag{36}$$

Equations (35) and (36) can be solved for T_i and r_i. The explicit solution for T_i under conditions of $2d \gg r_i$ is obtained from the quadratic equation

$$0.5(aT_i^2) + (b - k_d)T_i + [k_d T_w - bT_s - 0.5(aT_s^2) - r_i \ddot{q}_{cr} \ln(2d/R)] = 0. \tag{37}$$

Knowledge of the radius and temperature of the dry–moist interface permits calculations of the entire temperature field by the same technique outlined in this work.

The phenomenon of desiccation is undesirable since it inhibits soil warming. In necessary circumstances, desiccation could be avoided by proper management of irrigation frequency, adoption of intermittent heating schedules and use of adequate water tables [4].

APPENDIX II

THE TEMPERATURE DEPENDENT SOIL THERMAL CONDUCTIVITY FUNCTION

The soil is considered as a medium which contains a continuous phase (liquid moisture) and a dispersion of $M-1$ constituents (solid particles and gas-filled pores). The thermal conductivity of the soil is given by

$$k = \left(\sum_{i=0}^{M} J_i \omega_i k_i\right) \Big/ \sum_{i=0}^{M} J_i \omega_i, \tag{38}$$

where k_i is the thermal conductivity of the ith constituent, ω_i its volume fraction, and J_i the space average ratio of temperature gradients in the ith constituent to that of the continuum. Assuming that the dispersed constituents are spheroidal in shape and randomly oriented, J_i is described by

$$J_i = \frac{1}{3} \sum_{j=l,m,n} \left[1 + \left(\frac{k_i}{k_0} - 1\right) g_{i,j}\right]^{-1}, \tag{39}$$

where k_0 denotes the thermal conductivity of the continuum, l, m, n the spheroid axes, and $g_{i,j}$ geometric shape factors, equivalent to the depolarization factors in the theory of dielectrics. The sum of these factors is unity, $g_{i,l}+g_{i,m}+g_{i,n} = 1$, and $g_{i,l} = g_{i,m}$. They can be determined theoretically or experimentally [9, 10].

Different equations are used for the evaluation of J_i, depending on the soil moisture content. In the range of moisture content between field capacity and saturation, the apparent thermal conductivity of the gas filled pores is

$$k_{app} = k_a + k_v^s. \tag{40}$$

The term k_v^s is essentially the apparent thermal conductivity of the vapour phase due to latent heat transport. Driven by temperature gradients, moisture evaporation, diffusion and recondensation appears as a powerful mechanism of latent heat transfer within the pore space. The evaluation of k_v^s is based on Fick's law, applied for diffusion of saturated vapour [9]. In the range of moisture content between wilting point and field capacity, the vapour phase cannot be considered as saturated. For this range, the apparent conductivity is approximated by

$$k_{app} = k_a + \phi k_v^s = k_a + \frac{\omega_w}{\omega_f} k_v^s. \tag{41}$$

A value of 0.144 was assigned to the shape factors ($g_{1,l}$ and $g_{2,l}$) of the considered sand and organic solid particles, corresponding to spheroids with axes $l = m = 4n$. The shape factor of the gas filled pores depends on moisture content. For the range $\omega_f \leqslant \omega_w \leqslant \omega_w^s$, the following expression is used

$$g_{3,l} = 0.333 - \frac{\omega_a}{\omega_w^s}\left[0.333 - (g_{3,l})_{\omega_w \to 0}\right]. \tag{42}$$

The calculation of $g_{3,l}$ for desiccated conditions ($\omega_w \to 0$) is based on the knowledge that the particles are weakly wetted and $g_{w,l} = 0.144$, considering the gas as a continuum. Assigning the thermal conductivity of water to the particles, one obtains a parameter J_w which equals $1/J_{gas}$ of the same medium with water as a continuum [9]. The value of $g_{3,l}$ that corresponds to J_{gas} with $k_{app} = k_a + k_v^s$ and $k_0 = k_w$ is the shape factor of gas-filled pores of a nearly dry soil. The equation describing $g_{3,l}$ in the range of $0 \leqslant \omega_w < \omega_f$ is

$$g_{3,l} = 0.013 + \frac{\omega_w}{\omega_f}\left[(g_{3,l})_{\omega_w = \omega_f} - 0.013\right].$$

The thermal conductivities of the quartz sand and organic particles, used in the calculation, are 8.16 and 2.93 W m^{-1} °C^{-1}, respectively. Calculated values of the soil thermal conductivities are shown in Fig. 5. It is seen that these values can be represented fairly well by a linear function, equation (34).

DISTRIBUTION DE TEMPERATURE AUTOUR D'UN RESEAU DE TUBES ENTERRES, AVEC CONDUCTIVITE THERMIQUE FONCTION DE LA TEMPERATURE

Résumé—On étudie la distribution de température dans le sol autour d'un réseau de tubes horizontaux, enterrés et parcourus par de l'eau chaude. Des calculs de la conductivité thermique du sol révèlent une dépendance linéaire vis-à-vis de la température, due à la présence d'humidité et à la diffusion de vapeur dans les pores. Des solutions du champ de température autour des différents réseaux de tubes sont obtenues sont forme analytiques et numériques. Des expériences concernent un seul tube enterré. Les résultats montrent que le présent modèle donne de meilleures prédictions que les modèles antérieurs à propriétés constantes. Des analyses sont étendues pour tenir compte des effets de la dessiccation autour des tubes chauffés. Les résultats sont applicables en horticulture pour le calcul des réseaux performants de chauffage du sol.

TEMPERATURVERTEILUNG IN DER UMGEBUNG VON ROHRGITTERN, DIE IN DEN BODEN EINGEGRABEN SIND, UNTER BERÜCKSICHTIGUNG DER TEMPERATURABHÄNGIGEN WÄRMELEITFÄHIGKEIT

Zusammenfassung—Die Temperaturverteilung im Boden um ein unterirdisches Netzwerk aus horizontalen Warmwasserleitungen wurde untersucht. Berechnungen der Wärmeleitfähigkeit des Bodens zeigten eine lineare Temperaturabhängigkeit, die durch die Anwesenheit von Feuchtigkeit und durch induzierte Dampfdiffusion innerhalb des porösen Bodens verursacht ist. Für die Temperaturverteilung in der Umgebung verschiedener eingegrabener Leitungsnetze ergaben sich geschlossene und numerische Lösungen. Es wurden auch Versuche mit einem eingegrabenen Einzelrohr durchgeführt. Die Ergebnisse zeigten, daß das vorliegende Modell zu besseren Vorhersagen führt als bisherige Modelle mit konstanten Stoffdaten. Die Untersuchungen wurden ausgedehnt, um die Auswirkungen der Trocknung in der Umgebung beheizter Leitungen zu berücksichtigen. Die Ergebnisse sind bei der Verbesserung der Auslegung von Bodenerwärmungsgittern im Gartenbau anwendbar.

РАСПРЕДЕЛЕНИЕ ТЕМПЕРАТУР В ОКРЕСТНОСТЯХ ПОДЗЕМНОЙ ВОДОПРОВОДНОЙ СЕТИ В ПОЧВЕ С ТЕПЛОПРОВОДНОСТЬЮ, ЗАВИСЯЩЕЙ ОТ ТЕМПЕРАТУРЫ

Аннотация—Исследовано температурное поле в почве в окрестностях сети подземных горизонтальных труб с теплой водой. При расчетах использована линейная зависимость теплопроводности почвы от температуры, обусловленная влажностью и вызванной ею диффузией пара в порах. Решения уравнений теплопроводности вокруг различных подземных водопроводных сетей найдены в замкнутом виде. Эксперименты проводились с одной подземной трубой. Результаты показали, что данная модель описывает процессы точнее, чем ранее известные модели, предполагающие свойства постоянными. Анализ распространен на случай учета эффектов сушки вокруг нагретых труб. Результаты можно применять в садоводстве для усовершенствования конструкций сетей подогрева почвы.